Physics Letters B 808 (2020) 135676

Contents lists available at ScienceDirect

Physics Letters B

www.elsevier.com/locate/physletb

Basis-dependent measures and analysis uncertainties in nuclear chaoticity

Long-Jun Wang [a,*], Fang-Qi Chen [b], Yang Sun [c]

[a] School of Physical Science and Technology, Southwest University, Chongqing 400715, China
[b] Department of Applied Physics, School of Science, Northwestern Polytechnical University, Xi'an 710129, China
[c] School of Physics and Astronomy, Shanghai Jiao Tong University, Shanghai 200240, China

ARTICLE INFO

Article history:
Received 28 April 2020
Received in revised form 28 July 2020
Accepted 30 July 2020
Available online 5 August 2020
Editor: W. Haxton

Keywords:
Quantum chaos
Information entropy
Spectral statistics
Odd-mass nuclei
Angular-momentum projection

ABSTRACT

Chaoticity in nuclei is usually measured by the information entropy through analyzing wave functions, or by spectral statistics with the spectral rigidity and the nearest neighbor level spacing (NNLS) distribution. We show that although information entropy (or localization length) is a basis-dependent quantity, it is helpful for understanding the complexity of wave functions, especially when the corresponding levels lie in a highly-excited, dense region. On the other hand, although nuclear levels used for spectral statistics are quantum-mechanically observable, one has to treat them through a model- (and parameter-) dependent unfolding procedure, which may introduce large uncertainties for drawing a conclusion. By applying the projected shell model, we address these problems with an ensemble of $\sim$ 20,000 $J^{\pi} = 1/2^{+}$ levels calculated for the well-deformed, odd-mass nucleus ^{153}Nd. Residual interactions that are responsible for nuclear chaoticity are discussed as well.

In nuclear spectra from the ground state up to high excitation energy regime with high level density, the property of nuclear levels changes with appearance of specific structures. Near the ground state (of even-even nuclei, typically) with all nucleons being paired, the levels are characterized mainly as the collective rotation and vibrations [1]. Soon after the first nucleon-pair breaking at the energy of 2Δ (pairing gap, with $\Delta \approx 1$ MeV typically), the system enters into a regime determined by the interplay between the collective and quasiparticle (qp) excitations. As excitation energy goes further up, more and more nucleon pairs are broken, and the system begins to show clear signs of qp's in chaotic motion [2,3]. The features of the complicated dynamics in a chaotic nuclear system are controlled by residual interactions of qp's. The actual stationary states become extremely complicated superpositions of the original simple configurations. Zelevinsky et al. call this process 'stochastization' [4]. At the ultra-high spin and excitation regime, new kinds of collective excitations can emerge when the old organizations have been completely destroyed [5]. In addition to the spectroscopic problems, there has been an interesting, but unsolved problem on the widths of neutron resonances. This question was discussed by Volya et al. (see Ref. [6] and the references therein), and by E. Bogomolny in a following paper [7] to improve the mathematical treatment. However, the final solution must involve detailed calculations for heavy, deformed nuclei.

Study of chaoticity in nuclei is not only of theoretical interest, but can also have important implications if the nuclei are exposed to high-temperature environments. Nuclear level densities are known to play an essential role in the calculation of reaction cross sections applied to astrophysical nucleosynthesis studies, nuclear energy production, and transmutation of nuclear waste. However, as the number of nuclear levels increases exponentially with excitation energy, typically for the rare earth region, the level density changes by a factor of one million when going from the ground state up to the neutron binding energy [8]. Understanding of such a huge ensemble of quantum levels in strongly-correlated quantum systems is a great challenge.

For the highly-excited nuclear states, the empirical information available on the structure of wave functions is rather limited. In most prevailing nuclear models, the multidimensional configuration space is usually far from being sufficient for a quantitative discussion about the stochastization. Instead, one has to work with the states in very restricted Hilbert space. Such models are not very useful for understanding chaotic dynamics in actual many-body systems where the approximation of isolated single-particle or collective degrees of freedom becomes invalid very quickly as the excitation energy increases [4].

In Ref. [4], Zelevinsky et al. carried out a pioneering research with realistic calculations. They reported the first results of the

* Corresponding author.
E-mail addresses: longjun@swu.edu.cn (L.-J. Wang), sunyang@sjtu.edu.cn (Y. Sun).

https://doi.org/10.1016/j.physletb.2020.135676

analysis of eigenvalues and the eigenvectors of the nuclear shell model from the viewpoint of order, chaos, complexity and thermalization. Energy levels and wave functions were used to study quantum chaos and complexity of nuclear systems. The degree of complexity of wave functions was measured by the information entropy of the components. It was emphasized that the measures with information entropy depend sensitively on the representation. The construction of basis states with exact quantum numbers of angular momentum and isospin is important for the study. Nevertheless, their shell-model valence space [4] is restricted to one major shell (24 valence states in the *sd*- or 40 in the *fp*-shell), which is still rather limited.

In the present work, we study quantum chaos and complexity with realistic nuclear structure calculations by the projected shell model (PSM) [9]. The PSM is a shell model for heavy, deformed nuclei, practically with no restriction to the size of valence single-particle space. It can therefore be applied even to the heaviest nuclei [10] corresponding to systems at the extreme of level density. The aim of the present investigation is twofolds. First, in a typical PSM calculation, it takes several transformations among different bases. This provides us with possibilities to discuss the complexity in a realistic calculation by writing the wave functions in different representations. Through the study of the localization length, we can extract useful information for the complexity. Second, we take the advantage of having a large number of levels with definite angular momentum and parity to perform statistical analysis. We touch upon a question occurring in every detailed spectral statistical analysis, i.e. uncertainties caused by the unfolding procedure. We take the odd-neutron nucleus ^{153}Nd as the example. Odd-mass nuclei, having on average 5 - 7 times more levels than their even-even partners, are optimal for such study since many levels exist already at low-lying regions. However, chaoticity in odd-mass nuclei is seldom investigated.

Like a conventional shell model, a PSM calculation starts with an effective shell-model Hamiltonian $\hat{H}$ that consists of the one-body (mean field) part $\hat{H}_0$ and the residual interaction $\hat{H}'$ of the two-body type:

$$\hat{H} = \hat{H}_0 + \hat{H}'. \tag{1}$$

The essential difference between the PSM and conventional shell models lies in the way of construction of shell model configuration space. Unlike a conventional way of building many-body configurations by direct couplings of angular momenta, the PSM first transforms the representation from the spherical basis to the intrinsic frame described by a deformed Nilsson mean field [11]. Pairing correlations are treated by the BCS method for the deformed single-particle states obtained from the Nilsson calculation [9]. These correspond to two successive transformations: (1) a unitary transformation of particles defined in the original spherical basis to those in a deformed basis, and (2) a Bogoliubov-type transformation that changes deformed single-particle states to qp states [1]. Note that the resulting qp basis with a properly chosen deformation should be very close to the 'true' deformation of a nucleus. Through these operations, the deformed qp basis incorporates efficiently important correlations through the concept of spontaneous symmetry breaking in the spacial and gauge fields [12].

Working with the deformed qp basis, we can now construct multi-qp configurations. For odd-neutron nuclei, we have

$$\Big\{ \hat{a}^\dagger_{\nu_i}|\Phi\rangle,\ \hat{a}^\dagger_{\nu_i}\hat{a}^\dagger_{\nu_j}\hat{a}^\dagger_{\nu_k}|\Phi\rangle,\ \hat{a}^\dagger_{\nu_i}\hat{a}^\dagger_{\pi_j}\hat{a}^\dagger_{\pi_k}|\Phi\rangle,\ \hat{a}^\dagger_{\nu_i}\hat{a}^\dagger_{\nu_j}\hat{a}^\dagger_{\nu_k}\hat{a}^\dagger_{\pi_l}\hat{a}^\dagger_{\pi_m}|\Phi\rangle \Big\}, \tag{2}$$

where $\hat{a}^\dagger_\nu$ ($\hat{a}^\dagger_\pi$) labels neutron (proton) qp creation operator associated with the qp vacuum $|\Phi\rangle$. These multi-qp configurations are written in the spirit of the Tamm-Dancoff method [1], with each term having a well-defined physical meaning. For example, if $\hat{a}^\dagger_{\nu_i}|\Phi\rangle$ describes the low-lying neutron single particle states, $\hat{a}^\dagger_{\nu_i}\hat{a}^\dagger_{\nu_j}\hat{a}^\dagger_{\nu_k}|\Phi\rangle$ ($\hat{a}^\dagger_{\nu_i}\hat{a}^\dagger_{\pi_j}\hat{a}^\dagger_{\pi_k}|\Phi\rangle$) describes states with one broken neutron (proton) pair. In the present work, up to 5-qp states are included as in Ref. [13].

The configurations in Eq. (2) are based on deformed qp-states in the intrinsic frame, which violate rotational symmetry. There is the well-established numerical method to restore the rotational symmetry by applying exact angular-momentum projection operator to the configurations

$$\hat{P}^I_{MK} = \frac{2I+1}{8\pi^2}\int d\Omega D^I_{MK}(\Omega)\hat{R}(\Omega), \tag{3}$$

which is defined with the Euler angle Ω, the rotation operator $\hat{R}$, and the Wigner D-function D^I_{MK} [14]. The PSM wave functions in the laboratory system can be expanded as superposition of the (angular-momentum) projected multi-qp configurations in Eq. (2) (denoted by $|\Phi_\kappa\rangle$),

$$|\Psi^\omega_{IM}\rangle = \sum_{K\kappa} F^\omega_{IK\kappa}\hat{P}^I_{MK}|\Phi_\kappa\rangle. \tag{4}$$

The expansion coefficients $F^\omega_{IK\kappa}$ are obtained by diagonalizing the Hamiltonian numerically. i.e., by solving the Hill-Wheeler-Griffin equation,

$$\sum_{\kappa' K'}\Big(H^I_{K\kappa,K'\kappa'} - E^\omega_I N^I_{K\kappa,K'\kappa'}\Big)F^\omega_{IK'\kappa'} = 0, \tag{5}$$

with the projected matrix elements for the Hamiltonian and the norm,

$$H^I_{K\kappa,K'\kappa'} = \langle\Phi_\kappa|\hat{H}\hat{P}^I_{KK'}|\Phi_{\kappa'}\rangle, \tag{6a}$$

$$N^I_{K\kappa,K'\kappa'} = \langle\Phi_\kappa|\hat{P}^I_{KK'}|\Phi_{\kappa'}\rangle. \tag{6b}$$

It should be noted that the above norm matrix is not an identity matrix as in a usual eigenvalue equation, indicating that the projected basis in Eq. (4) is non-orthonormal. The rotational-invariant two-body Hamiltonian in terms of separable forces is adopted

$$\hat{H} = \hat{H}_0 - \frac{\chi}{2}\sum_\mu \hat{Q}^\dagger_{2\mu}\hat{Q}_{2\mu} - G_M\hat{P}^\dagger\hat{P} - G_Q\sum_\mu \hat{P}^\dagger_{2\mu}\hat{P}_{2\mu} + \hat{H}_{\rm GT}, \tag{7}$$

which includes the one-body term, the quadrupole-quadrupole interaction, the monopole-pairing interaction, the quadrupole-pairing interaction, and the two-body Gamow-Teller (GT) force (see Ref. [13] for more details). We stress that our Hamiltonian does not contain any random elements. The chaoticity, if any, arises naturally as a result of strong mixing of the configurations by residual interactions.

In addition to the non-orthonormal projected basis in Eq. (4), the projection calculation involves two more bases to express the PSM wave functions. One is the orthonormal mixing basis

$$|W_\sigma\rangle \equiv \frac{1}{\sqrt{n_\sigma}}\sum_{K\kappa} U^\sigma_{K\kappa}\hat{P}^I_{MK}|\Phi_\kappa\rangle, \tag{8}$$

where n_σ ($U^\sigma_{K\kappa}$) labels the eigenvalue (eigenvector) of the norm matrix in Eq. (6b). The PSM wave functions can be expressed as (see Appendix),

$$|\Psi^\omega_{IM}\rangle = \sum_{\sigma,\ n_\sigma\neq 0} V^{I\omega}_\sigma|W_\sigma\rangle. \tag{9}$$

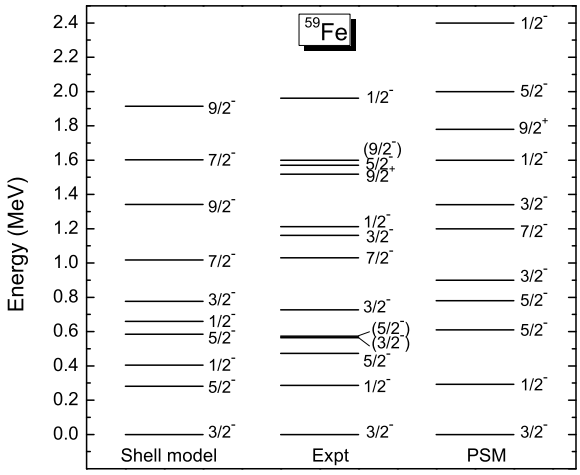

Fig. 1. The calculated energy levels for ^{59}Fe [15] as compared with the data [16] and shell-model calculations [17].

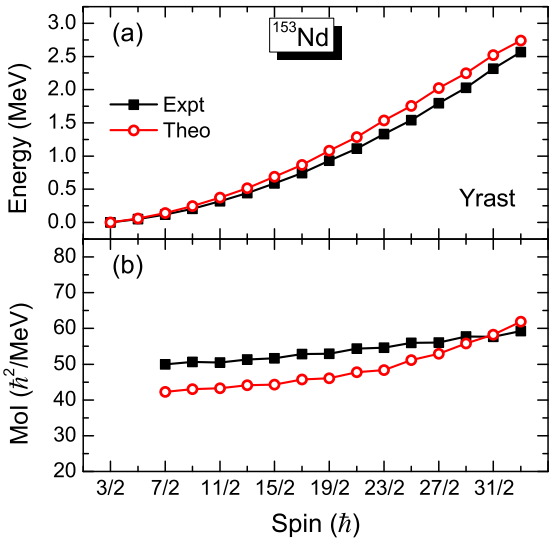

Fig. 2. The calculated energy levels and the moments of inertia for the yrast band of ^{153}Nd, as compared with the data [22].

The other is the orthonormal intrinsic qp basis $|K\kappa\rangle$, which is constructed based on Eq. (2), so that the PSM wave functions can also be written as (see Appendix for derivation)

$$|\Psi^{\omega}_{IM}\rangle = \sum_{K\kappa} g^{I\omega}_{K\kappa}|K\kappa\rangle. \tag{10}$$

Thus the wave functions in a projection theory can be expressed in terms of Eqs. (4), (9) and (10). Note that these bases are very different from the conventional shell model basis (such as those in Ref. [4]), although they all can represent the same shell-model wave functions. Besides, it can be seen from Eqs. (4), (9), (10) and (20) that in the cases of three different bases, the angular momentum is conserved through exact angular-momentum projection.

Before discussing statistic features of nuclear systems, we first demonstrate that the PSM as an unconventional shell model can indeed well describe the basic nuclear properties. The pf-shell nuclei are the examples for which conventional shell-model calculations are still feasible. In Fig. 1, we compare the PSM calculation for a typical pf-shell nucleus, ^{59}Fe [15] with the experimental data [16] as well as the shell-model calculation using the GXPF1A interaction [17]. It can be seen that PSM can describe the experimental levels equally well as the conventional shell model. The PSM has been tested for other pf-shell nuclei, for example, in Refs. [18–20].

We use the information entropy to measure the complexity of nuclear wave function, which is calculated as [4,21]

$$I_H(\alpha) = \sum_{i=1}^{d} -|X^{\alpha}_i|^2 \ln(|X^{\alpha}_i|^2). \tag{11}$$

In Eq. (11), X^{α}_i can be $F^{\omega}_{IK\kappa}$ in Eq. (4) of the non-orthonormal projected basis (termed as F-basis hereafter), or $V^{I\omega}_{\sigma}$ in Eq. (9) of the orthonormal mixing basis (V-basis), or $g^{I\omega}_{K\kappa}$ in Eq. (10) of the orthonormal intrinsic qp basis (g-basis). d in Eq. (11) is the dimension of the corresponding basis. For the GOE matrices (limit), $\langle I_H\rangle = \ln(0.48d)$. To avoid the dimension dependence of I_H, the normalized localization length l_H is introduced [4,21]

$$l_H(\alpha) = \frac{\exp(I_H(\alpha))}{0.48d}. \tag{12}$$

Our discussion on the information entropy employs the heavy, deformed odd-neutron nucleus ^{153}Nd, for which all parameters in the PSM calculations are adopted exactly as those in Ref. [13], which means it is a realistic calculation that can well reproduce both low-lying and high-lying states, as well as the known GT transitions [13]. The employed valence space is large as compared to a one-major shell model: three major harmonic shells with $N = 4, 5, 6$ ($N = 3, 4, 5$) are taken for neutrons (protons). It is important to work in a large, multi-shell basis to analyze chaoticity to avoid any artificial conclusions due to space limit. The quadrupole and hexadecapole deformation parameters are adopted as $\varepsilon_2 = 0.250$ and $\varepsilon_4 = -0.073$ taken from Ref. [23], for the construction of the deformed single-particle basis. Before the analysis of the information entropy, we show in Fig. 2 the calculated energy levels and moments of inertia (MoI) for the yrast band of ^{153}Nd, and compared them with the data [22]. As one can see, both quantities are described nicely by the calculation, indicating that the PSM is a realistic model for heavy, deformed nuclei.

Fig. 3 shows the calculated l_H for the above-mentioned three bases from an ensemble of $\sim$ 20,000 $1/2^+$ states in ^{153}Nd, from the ground state to excitations beyond 20 MeV. It is seen from Fig. 3(a) that the localization length l_H (or information entropy) shows very sensitive basis-dependence. The calculated l_H with the wave functions from the three bases have totally different distributions. For the results with the F-basis (filled squares in Fig. 3(a)), no useful information about complexity can be extracted because for most states in the ensemble, l_H is practically zero (less than 10^{-10}). There are some scattered points in space with a few exceeding the GOE limit, which are unmeaningful. This means that the condition of orthonormality for the bases is indispensable if the wave functions are used for analyzing the information entropy. It is known that non-orthonormality in wave functions is a general consequence of the Hill-Wheeler-Griffin equation, and the wave functions (in the F-basis) from the (angular-momentum) projection theory do not represent probability [9].

For the two orthonormal bases, the g-basis corresponds to the intrinsic multi-qp basis $|K\kappa\rangle$. Since ^{153}Nd has a prolate shape with stable deformation, a resulting $\varepsilon_2 \approx 0.25$ [23–25] from variational calculations coincides approximately with the 'true' deformation of ^{153}Nd. As discussed before, each multi-qp configuration (i.e. those in Eq. (2)) constructed from such a 'good' mean-field has a clear physical meaning [12]. The calculated l_H's in the g-basis are all small (see Fig. 3(a), open triangles), suggesting that the states are localized in $|K\kappa\rangle$ of the g-basis. Physically, wave functions of low-lying (higher-lying) states take major components from the lower-order qp (higher-order qp) configurations. On the other hand, the orthonormal V-basis mixes the projected multi-qp configurations. The mixing coefficients are given by $U^{\sigma}_{K\kappa}$ in Eq. (8). The l_H's calculated in this basis (open circles in Fig. 3(a)) tend to be more

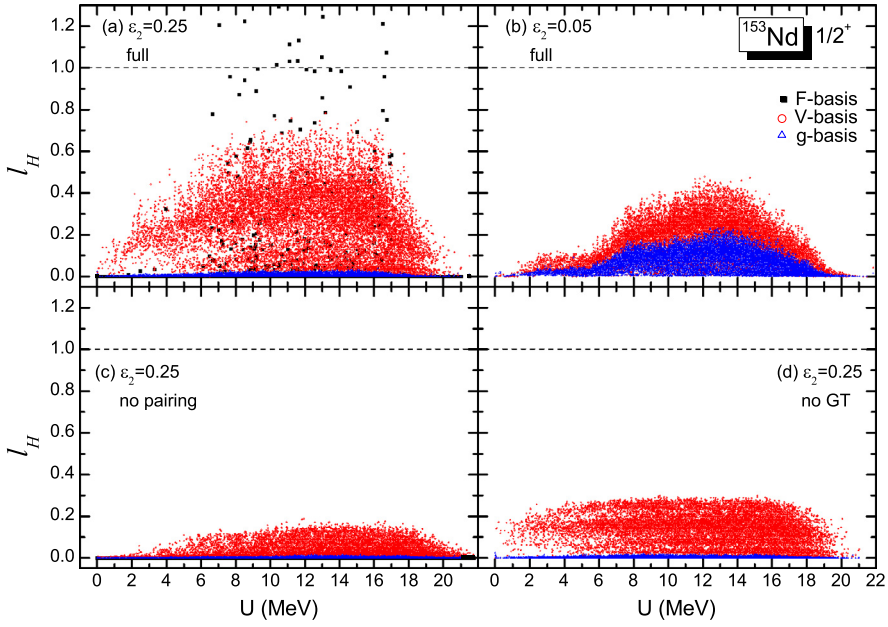

Fig. 3. The localization length l_H of about 20,000 $1/2^+$ states for ^{153}Nd as a function of excitation energy above the yrast state, in terms of different bases for different cases (the deformation of bases and the Hamiltonian). The dashed line indicates $l_H = 1$, corresponding to the GOE (totally chaotic) limit.

delocalized as compared with those in the g-basis, and have a generic Gaussian energy-dependence. In the most chaotic (middle) part of the spectrum, the l_H's have an average value around 0.4. The maximum l_H lie at ~ 0.7, which does not reach the GOE limit. It should be pointed out that the degree of delocalization depends on the nature of the projected basis. The more the norm matrix (see Eq. (6)) departures from the identity matrix, the higher the degree of delocalization.

The above discussions have explored in some depth the basis-dependent measures of information entropy in the PSM calculation. We can further analyze the basis dependence feature of l_H by changing the basis deformation. We construct the single-particle basis with deformation parameter $\varepsilon_2 = 0.05$, corresponding to a (near) spherical single-particle basis, while keeping all other calculation conditions the same as in Fig. 3(a). With a near-zero deformation, the g-basis expressed by $|K\kappa\rangle$ is now far from that with the 'true' deformation, and thus the so-calculated l_H's through $g^{I\omega}_{K\kappa}$ of Eq. (10) are more delocalized, as seen in Fig. 3(b). For the V-basis with a near-zero deformation, $|W_\sigma\rangle$ in Eq. (9) should be close to $|K\kappa\rangle$ because a PSM basis with a small deformation approaches the (spherical) shell-model basis. Indeed, it is seen from Fig. 3(b) that the l_H distributions in the V- and g-bases exhibit similar energy dependence, with differences only in magnitude, showing a better Gaussian behavior as in conventional shell model calculations [4,26].

Quantum chaos is expected to set in when the level density is sufficiently high and levels are strongly mixed by residual interactions [3,4]. An interesting question is which types of residual interaction play major roles for the emerging chaoticity [27,5]. One advantage of adopting separable forces in the Hamiltonian is that the roles of individual residual forces can be easily detected, as illustrated in the study of neutrinoless double beta decay [28]. In Figs. 3(c) and (d), we show the energy dependence of l_H in two additional calculations: one without the pairing forces (by setting $G_M = G_Q = 0$ in Eq. (7)) and the other without the GT force (by removing $\hat{H}_{\rm GT}$ in Eq. (7)). The resulting l_H's for the g-basis are all small in Figs. 3(c) and (d). This is expected already in Fig. 3(a), which can be understood as for a basis with its deformation close to the 'real' situation, residual interactions are no longer significant in configuration mixing. However, very different result is found for the V-basis. As seen from Fig. 3(c), l_H without pairing correlations decreases considerably, indicating that the pairing plays a role in enhancing chaoticity for both low- and high-energy regions. Such conclusion is drawn in Ref. [4], and is also consistent with that obtained by analyzing electro-magnetic transitions [5]. In Ref. [29], the chaoticity of quantum states in a two-dimensional pairing model with a contact pairing force as the two-body interaction is found to increase rapidly when the pairing strength grows from zero, which is very similar to our conclusion as seen from Fig. 3(a) and (c). Interestingly, the chaoticity of quantum states turns out to decrease with the pairing strength when the pairing strength is very large, as seen from the Fig. 6 of Ref. [29]. On the other hand, the comparison of Figs. 3(d) and (a) reveals that for nuclear levels in the middle range of the spectrum where the level density is high, a residual GT force that acts in the spin-isospin channel enhances the chaoticity. The dependence of quantum chaos in nuclear structure on residual interactions has been discussed in shell model studies [30].

In the above discussions, quantum chaos and complexity are discussed in terms of wave functions, which are not directly observable. Quantum chaos can also be measured by spectral statistical analysis [31], where the NNLS distributions $P(s)$ and the spectral rigidity Δ_3 are usually the quantities, provided that the spectrum is unfolded first to separate the fluctuating part from the smooth part. The principal technique used for unfolding is to calculate the mean level density $\bar{\rho}(E)$, which is usually estimated by the local unfolding method,

$$\bar{\rho}(E_i) = \frac{2\nu}{E_{i-\nu} - E_{i+\nu}}, \tag{13}$$

where a set of neighboring levels in a window of ν levels on each side of E_i is considered. Or one uses a more sophisticated Gaussian broadening unfolding method,

$$\bar{\rho}(E) = \frac{1}{\eta\sqrt{2\pi}} \sum_i \exp\left\{ -\frac{(E - E_i)^2}{2\eta^2} \right\}, \tag{14}$$

where the sum runs over levels in the window of 2η effectively. With $\bar{\rho}(E)$, one obtains dimensionless unfolded energy levels, from which $P(s)$ and $\Delta_3(L)$ can be calculated in standard ways [31,32].

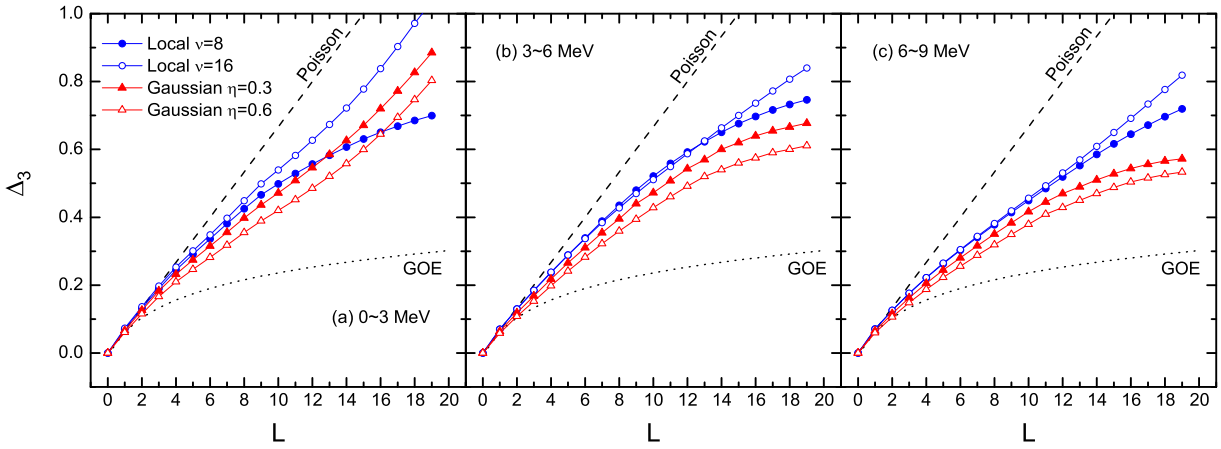

Fig. 4. The spectral rigidity Δ_3 at different excitation energy regions with different unfolding methods. The regular case (Poisson) and chaotic case (GOE) are illustrated correspondingly. For the Δ_3 which characterizes the long-range level correlations, the closer the results reach the GOE limit, the higher degree of chaoticity can be read.

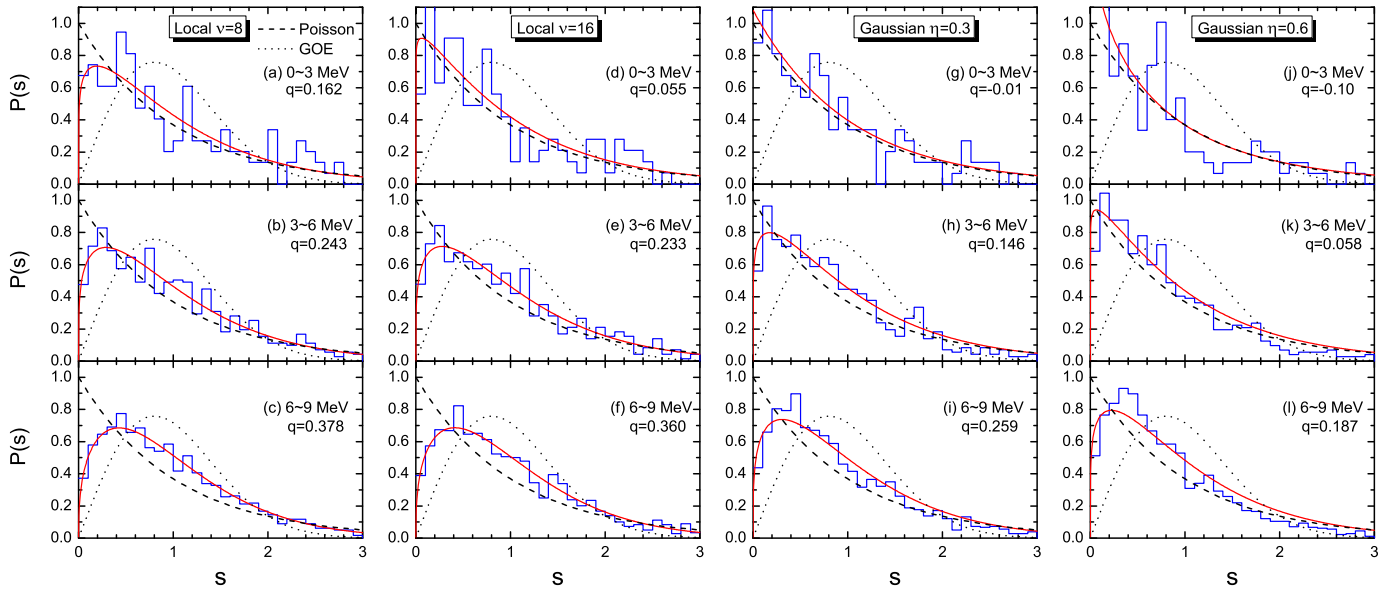

Fig. 5. The $P(s)$ (histogram) at different excitation energy regions with different unfolding methods. The best fitted Brody distribution (solid red line) is displayed with corresponding fitted parameter q.

The unfolding procedure is a nontrivial step for a statistic analysis. The unfolding methods haves been applied over decades [31–34,30,35,36], but the dependence on different methods and/or parameters has seldom been discussed. We show that for a same ensemble, the local unfolding and Gaussian broadening unfolding methods can bring *different* information on quantum chaos. Zelevinsky et al. realized this problem, and acknowledged in "Note added in proof" in their review article [4] that their results for the spectral rigidity Δ_3 are very sensitive to the details of the unfolding procedure.

To discuss uncertainties associated with unfolding, we again take ^{153}Nd as example as in Fig. 3(a) with an ensemble of ∼20,000 $1/2^+$ levels from diagonalization of the full Hamiltonian of Eq. (7). Figs. 4 and 5 show Δ_3 and $P(s)$, with collected levels from three different excitation regions (0-3, 3-6, 6-9 MeV). To illustrate influences with different unfolding methods and parameters in the methods, we vary the parameter ν in Eq. (13) or η in Eq. (14). For Δ_3 that characterizes long-range level correlations, a higher degree of chaoticity can be concluded for the system if the curve is closer to the GOE limit. It is seen from Fig. 4 that for smaller L, the dependence of the Δ_3 statistics on both the unfolding method and the unfolding procedure is not very large. However, the curves in Fig. 4 show larger departures from each other for larger L. For the local unfolding method as in Eq. (13), a *lower* degree of chaoticity is concluded if more levels are involved in the unfolding procedure, as one compares the results with $\nu = 8$ and $\nu = 16$ in Fig. 4. On the contrary, for the Gaussian broadening unfolding method in Eq. (14), a *higher* degree of chaoticity is concluded if more levels in a larger window of 2η are considered in the unfolding procedure, as one compares the results with $\eta = 0.3$ MeV and $\eta = 0.6$ MeV.

For the $P(s)$ distribution which measures the short-range correlations, the corresponding chaoticity is usually quantified in terms of a best fitted Brody distribution with a parameter q [37,21,33,36]. The Brody distribution reproduces the form of Poisson statistics that labels a regular system (with $q = 0$), and of the GOE distribution that labels a chaotic system (with $q \approx 0.95$). As seen from the different q-values in Figs. 5(a, d, g, j) or the corresponding $P(s)$ distribution (blue histogram), $P(s)$ shows some dependence on the unfolding method and procedure at lows excitation energy region ($0 \sim 3$ MeV). The dependence becomes weaker for higher excitation regions, as seen from the q-values or corresponding $P(s)$

distribution in the two lower panels in Fig. 5. It indicates that the NNLS distributions $P(s)$ might be a more reliable measure for spectral statistical analysis of nuclear systems, especially for higher excitation regions. The same conclusion has been found in analyzing the GOE level spectrum in Ref. [31].

In their recent publications, Zelevinsky and collaborators have emphasized [38,39] that shell model calculations invariably show the significant role of the matrix elements of the Hamiltonian which are not directly related to the global structure and collective motion. It was discussed that the effect occurs starting from some excitation energy after breaking a small number of pairs, and continues as the level density grows when mixing of close-in-energy-configurations becomes strong even with weak residual interactions. These parts of the interaction determine the finite lifetime of the simple quasiparticle (or collective) modes and their fragmentation in terms of complicated eigenstates of exceedingly entangled nature. They loosely characterized the contributions as responsible for the incoherent collision-like interactions which do not influence considerably the mean field and collective effects. However, these parts of the Hamiltonian contribute considerably to the level density making it smoother and increasing its Gaussian width [40,41]. At present it is not clear whether the PSM is an appropriate theory to address this question.

In summary, nuclear quantum chaos is expected to set in when the level density in an energy region is sufficiently high and the configurations that describe the levels are strongly mixed by residual interactions. One usually measures chaoticity in nuclei by using information entropy, or by studying spectral statistics with the spectral rigidity Δ_3 and the nearest neighbor level spacing distribution $P(s)$. Prior to our work, information entropy, which reflects complexity in nuclear wave functions, was discussed in terms of configurations constructed in spherical mean-field bases. In the present work, we have shown, for the first time, that a model based on the angular-momentum projection method can provide us with several uniquely-defined bases (orthonormal vs. non-orthonormal, intrinsic vs. laboratory frame, deformed vs. spherical). We have found very sensitive basis-dependence in measures of complexity, with a high chaoticity being concluded when the overlap between the 'true' nuclear states and the basis configurations is small.

Among the two types of spectral statistics analysis, the results from spectral rigidity Δ_3 using different unfolding methods and/or parameters are found to departure from each other very much, especially for large L. This could be dangerous for drawing a definite conclusion. The $P(s)$ distribution shows a weaker dependence on unfolding methods and/or parameters for higher excitation regions. However, for the lower excitation region (0-3 MeV) where the interplay between the collective and single-particle excitations dominates the physics, the conclusion on chaoticity has some dependence on unfolding. One may use other measures such as the transition strengths to obtain information about quantum chaos, although such quantities are usually very difficult to obtain experimentally, especially for highly excited states.

The nuclear pairing is found to be an important driving force for the system to become chaotic. Degrees of chaoticity are found to be sensitive to other residual interactions as well. In the most chaotic (middle) part of the spectrum, even a Gamow-Teller force acting on the spin-isospin channel can cause chaoticity.

The authors are sincerely grateful to the anonymous referee for helping in deepening the discussion and inspiring further studies, and to Dr. J. Dong for reading the manuscript. One of us (Y.S.) thanks Professor H. A. Weidenmüller for private communications. This work is supported by the Venture & Innovation Support Program for Chongqing Overseas Returnees (with Grant No. cx2019056), by the National Natural Science Foundation of China (with Grant Nos. 11905175, 11905172 and U1932206), and by the National Key Program for S&T Research and Development of China (No. 2016YFA0400501).

Declaration of competing interest

The authors declare that they have no known competing financial interests or personal relationships that could have appeared to influence the work reported in this paper.

Appendix A

The Hill-Wheeler-Griffin equation, Eq. (5), corresponds to an eigenvalue equation in the non-orthonormal projected basis $\hat{P}^I_{MK}|\Phi_\kappa\rangle$ (i.e., generally $N^I_{K\kappa,K'\kappa'} \neq 0$), which can be solved as follows. First, the norm matrix is diagonalized

$$\sum_{K'\kappa'} N^I_{K\kappa,K'\kappa'} U^\sigma_{K'\kappa'} = n_\sigma U^\sigma_{K\kappa}, \tag{15}$$

from which one can then construct the orthonormal mixing basis in Eq. (8), which fulfills

$$\langle W_\sigma | W'_{\sigma'} \rangle = \delta_{\sigma\sigma'}. \tag{16}$$

In the basis of $\{|W_\sigma\rangle, n_\sigma \neq 0\}$, the eigenvalue equation becomes [9]

$$G^I_{\sigma\sigma'} = \frac{1}{\sqrt{n_\sigma n_{\sigma'}}} \sum_{K\kappa K'\kappa'} U^\sigma_{K\kappa} H^I_{K\kappa,K'\kappa'} U^{\sigma'}_{K'\kappa'}, \tag{17}$$

$$\sum_{\sigma'} G^I_{\sigma\sigma'} V^{I\omega}_{\sigma'} = E^\omega_I V^{I\omega}_\sigma. \tag{18}$$

One can then get the energy E^ω_I and the eigenvector $V^{I\omega}_\sigma$ which corresponds to coefficient in terms of the mixing basis.

In order to write the nuclear wave functions in terms of orthonormal qp states which have clear physical picture (pure mean-field configuration) in the intrinsic system, we define $|K\kappa\rangle$ as the orthonormal eigen-state for different qp configuration generally,

$$\left|\Psi^\omega_{IM}\right\rangle = \sum_{K\kappa} \left|K\kappa\right\rangle \left\langle K\kappa \middle| \Psi^\omega_{IM}\right\rangle \equiv \sum_{K\kappa} g^{I\omega}_{K\kappa} \left|K\kappa\right\rangle. \tag{19}$$

To obtain the expression for $g^{I\omega}_{K\kappa}$, we note that

$$\begin{aligned} g^{I\omega}_{K\kappa} &= \langle K\kappa | \sum_{K'\kappa'} F^\omega_{IK'\kappa'} \hat{P}^I_{MK'} | \Phi_{\kappa'} \rangle \\ &= \sum_{K'\kappa'} F^\omega_{IK'\kappa'} \langle K\kappa | \hat{P}^I_{MK'} | \Phi_{\kappa'} \rangle, \end{aligned} \tag{20}$$

i.e., we need to know the expression for $\langle K\kappa|\hat{P}^I_{MK'}|\Phi_{\kappa'}\rangle$, which fulfills

$$\begin{aligned} &\sum_{K\kappa} \langle \Phi_{\kappa''} | \hat{P}^{I\dagger}_{MK''} | K\kappa \rangle \langle K\kappa | \hat{P}^I_{MK'} | \Phi_{\kappa'} \rangle \\ &= \langle \Phi_{\kappa''} | \hat{P}^I_{K''K'} | \Phi_{\kappa'} \rangle = N^I_{K''\kappa'',\, K'\kappa'}. \end{aligned} \tag{21}$$

If we define

$$\mathcal{N}^{1/2\ I}_{K\kappa K'\kappa'} \equiv \sum_\sigma U^\sigma_{K\kappa} \sqrt{n_\sigma} U^{\sigma *}_{K'\kappa'}, \tag{22}$$

one can prove that $\mathcal{N}^{1/2\ I}_{K\kappa K'\kappa'}$ fulfills all the relations like Eq. (21) that hold for $\langle K\kappa|\hat{P}^I_{MK'}|\Phi_{\kappa'}\rangle$, i.e. [42]

$$\mathcal{N}^{1/2\ I}_{K\kappa K'\kappa'} = \langle K\kappa | \hat{P}^I_{MK'} | \Phi_{\kappa'} \rangle. \tag{23}$$

Thus, we can obtain

$$
\begin{aligned}
g^{I\omega}_{K\kappa} &= \sum_{K'\kappa'} F^{\omega}_{IK'\kappa'} \mathcal{N}^{1/2\ I}_{K\kappa K'\kappa'} \\
&= \sum_{K'\kappa'} F^{\omega}_{IK'\kappa'} \sum_{\sigma} U^{\sigma}_{K\kappa} \sqrt{n_\sigma} U^{\sigma *}_{K'\kappa'} \\
&= \sum_{K'\kappa'} \sum_{\sigma',\ n_{\sigma'}\neq 0} \frac{V^{I\omega}_{\sigma'} U^{\sigma'}_{K'\kappa'}}{\sqrt{n_{\sigma'}}} \sum_{\sigma} U^{\sigma}_{K\kappa} \sqrt{n_\sigma} U^{\sigma *}_{K'\kappa'} \\
&= \sum_{\sigma\sigma',\ n_{\sigma'}\neq 0} \frac{V^{I\omega}_{\sigma'}}{\sqrt{n_{\sigma'}}} U^{\sigma}_{K\kappa} \sqrt{n_\sigma} \delta_{\sigma\sigma'} \\
&= \sum_{\sigma,\ n_\sigma \neq 0} V^{I\omega}_{\sigma} U^{\sigma}_{K\kappa}, \qquad (24)
\end{aligned}
$$

where we have used the expression $F^{\omega}_{IK\kappa} = \sum_{\sigma,\ n_\sigma\neq 0} \frac{V^{I\omega}_{\sigma} U^{\sigma}_{K\kappa}}{\sqrt{n_\sigma}}$ and the orthonormality of $U^{\sigma}_{K\kappa}$.

References

[1] P. Ring, P. Schuck, The Nuclear Many-Body Problem, Springer-Verlag, 1980.
[2] H.A. Weidenmüller, G.E. Mitchell, Random matrices and chaos in nuclear physics: nuclear structure, Rev. Mod. Phys. 81 (2009) 539.
[3] J.M.G. Gómez, K. Kar, V.K.B. Kota, R.A. Molina, A. Relano, J. Retamosa, Many-body quantum chaos: recent developments and applications to nuclei, Phys. Rep. 499 (2011) 103.
[4] V. Zelevinsky, B.A. Brown, N. Frazier, M. Horoi, The nuclear shell model as a testing ground for many-body quantum chaos, Phys. Rep. 276 (1996) 85.
[5] L.-J. Wang, J. Dong, F.-Q. Chen, Y. Sun, Projected shell model analysis of structural evolution and chaoticity in fast-rotating nuclei, J. Phys. G 46 (2019) 105102.
[6] A. Volya, H.A. Weidenmüller, V. Zelevinsky, Neutron resonance widths and the Porter-Thomas distribution, Phys. Rev. Lett. 115 (2015) 052501, https://doi.org/10.1103/PhysRevLett.115.052501.
[7] E. Bogomolny, Modification of the Porter-Thomas distribution by rank-one interaction, Phys. Rev. Lett. 118 (2017) 022501, https://doi.org/10.1103/PhysRevLett.118.022501.
[8] M. Guttormsen, et al., Experimental level densities of atomic nuclei, Eur. Phys. J. A 51 (2015) 170.
[9] K. Hara, Y. Sun, Projected shell model and high-spin spectroscopy, Int. J. Mod. Phys. E 4 (04) (1995) 637–785.
[10] R.-D. Herzberg, et al., Nuclear isomers in superheavy elements as stepping stones towards the island of stability, Nature 442 (2006) 896.
[11] S.G. Nilsson, C.F. Tsang, A. Sobiczewski, Z. Szymański, S. Wycech, C. Gustafson, I. Lamm, P. Möller, B. Nilsson, On the nuclear structure and stability of heavy and superheavy elements, Nucl. Phys. A 131 (1) (1969) 1–66.
[12] Y. Sun, Projection techniques to approach the nuclear many-body problem, Phys. Scr. 91 (2016) 043005.
[13] L.-J. Wang, Y. Sun, S.K. Ghorui, Shell-model method for Gamow-Teller transitions in heavy deformed odd-mass nuclei, Phys. Rev. C 97 (2018) 044302.
[14] D.A. Varshalovich, A.N. Moskalev, V.K. Khersonskii, Quantum Theory of Angular Momentum, World Scientific, 1988.
[15] L. Tan, Y.-X. Liu, L.-J. Wang, Z. Li, Y. Sun, A novel method for stellar electron-capture rates of excited nuclear states, Phys. Lett. B 805 (2020) 135432, https://doi.org/10.1016/j.physletb.2020.135432.
[16] M.S. Basunia, Nucl. Data Sheets 151 (2018) 1.
[17] A.N. Deacon, S.J. Freeman, R.V.F. Janssens, M. Honma, M.P. Carpenter, P. Chowdhury, T. Lauritsen, C.J. Lister, D. Seweryniak, J.F. Smith, S.L. Tabor, B.J. Varley, F.R. Xu, S. Zhu, Yrast structures in the neutron-rich isotopes ^{59,60}Fe and the role of the $g_{9/2}$ orbital, Phys. Rev. C 76 (2007) 054303, https://doi.org/10.1103/PhysRevC.76.054303.
[18] Y.-C. Yang, H. Jin, Y. Sun, K. Kaneko, Phys. Lett. B 700 (2011) 44.
[19] Y. Sun, Y.-C. Yang, H.-L. Liu, K. Kaneko, M. Hasegawa, T. Mizusaki, Projected shell model description for high-spin states in neutron-rich fe isotopes, Phys. Rev. C 80 (2009) 054306, https://doi.org/10.1103/PhysRevC.80.054306.
[20] Y. Sun, Y.-C. Yang, H. Jin, K. Kaneko, S. Tazaki, Projected shell model study for neutron-rich, odd-odd mn isotopes, Phys. Rev. C 85 (2012) 054307, https://doi.org/10.1103/PhysRevC.85.054307.
[21] R.A. Molina, J.M.G. Gómez, J. Retamosa, Energy and isospin dependence of nuclear chaos, Phys. Rev. C 63 (2000) 014311.
[22] G.S. Simpson, W. Urban, J.A. Pinston, J.C. Angelique, I. Deloncle, H.R. Faust, J. Genevey, U. Köster, T. Materna, R. Orlandi, A. Scherillo, A.G. Smith, J.F. Smith, T. Rząca-Urban, I. Ahmad, J.P. Greene, Near-yrast structure of n=93 neutron-rich lanthanide nuclei, Phys. Rev. C 81 (2010) 024313, https://doi.org/10.1103/PhysRevC.81.024313.
[23] P. Möller, J.R. Nix, W.D. Myers, W.J. Swiatecki, Nuclear ground-state masses and deformations, At. Data Nucl. Data Tables 59 (2) (1995) 185–381.
[24] P. Möller, A.J. Sierk, T. Ichikawa, H. Sagawa, Nuclear ground-state masses and deformations: Frdm(2012), At. Data Nucl. Data Tables 109–110 (2016) 1.
[25] Y. Kuang, Z.P. Li, Private communication.
[26] M. Horoi, B.A. Brown, V. Zelevinsky, Random versus realistic interactions for low-lying nuclear spectra, Phys. Rev. Lett. 87 (2001) 062501.
[27] A. Bracco, S. Leoni, High-lying collective rotational states in nuclei, Rep. Prog. Phys. 65 (2002) 299.
[28] J. Menéndez, N. Hinohara, J. Engel, G. Martínez-Pinedo, T.R. Rodríguez, Testing the importance of collective correlations in neutrinoless double beta decay, Phys. Rev. C 93 (2016) 014305.
[29] J.R. Armstrong, S. Åberg, S.M. Reimann, V.G. Zelevinsky, Complexity of quantum states in the two-dimensional pairing model, Phys. Rev. E 86 (2012) 066204, https://doi.org/10.1103/PhysRevE.86.066204.
[30] B. Dietz, A. Heusler, K.H. Maier, A. Richter, B.A. Brown, Chaos and regularity in the doubly magic nucleus ^{208}Pb, Phys. Rev. Lett. 118 (2017) 012501.
[31] J.M.G. Gómez, R.A. Molina, A. Relano, J. Retamosa, Misleading signatures of quantum chaos, Phys. Rev. E 66 (2002) 036209.
[32] D. Mulhall, Z. Huard, V. Zelevinsky, Ergodicity of the δ_3 statistic and purity of neutron resonance data, Phys. Rev. C 76 (2007) 064611.
[33] S. Karampagia, D. Bonatsos, R.F. Casten, Regularity and chaos in 0^+ states of the interacting boson model using quantum measures, Phys. Rev. C 91 (2015) 054325.
[34] L. Munoz, A. Relano, Spectral-statistics properties of the experimental and theoretical light baryon and meson spectra, Phys. Rev. C 92 (2015) 035207.
[35] B. Dietz, B.A. Brown, U. Gayer, N. Pietralla, V.Y. Ponomarev, A. Richter, P.C. Ries, V. Werner, Chaos and regularity in the spectra of the low-lying dipole excitations of ^{50}Cr, Phys. Rev. C 98 (2018) 054314.
[36] A.P. Severyukhin, S. Åberg, N.N. Arsenyev, R.G. Nazmitdinov, Damped transient response of the giant dipole resonance in the lead region, Phys. Rev. C 98 (2018) 044319.
[37] T.A. Brody, J. Flores, J.B. French, P.A. Mello, A. Pandey, S.S.M. Wong, Random-matrix physics: spectrum and strength fluctuations, Rev. Mod. Phys. 53 (1981) 385.
[38] V.G. Zelevinsky, D. Mulhall, A. Volya, Do we understand the role of incoherent interactions in many-body physics?, Phys. At. Nucl. 64 (2001) 525, https://doi.org/10.1134/1.1358477.
[39] F. Borgonovi, F.M. Izrailev, L.F. Santos, V.G. Zelevinsky, Quantum chaos and thermalization in isolated systems of interacting particles, Phys. Rep. 626 (2016) 1, https://doi.org/10.1016/j.physrep.2016.02.005, http://www.sciencedirect.com/science/article/pii/S0370157316000831.
[40] R. Sen'kov, V. Zelevinsky, Nuclear level density: shell-model approach, Phys. Rev. C 93 (2016) 064304, https://doi.org/10.1103/PhysRevC.93.064304.
[41] V. Zelevinsky, M. Horoi, Nuclear level density, thermalization, chaos, and collectivity, Prog. Part. Nucl. Phys. 105 (2019) 180, https://doi.org/10.1016/j.ppnp.2018.12.001, http://www.sciencedirect.com/science/article/pii/S0146641018301029.
[42] Y. Sun, C.-L. Wu, K. Bhatt, M. Guidry, SU(3) symmetry and scissors mode vibrations in nuclei, Nucl. Phys. A 703 (2002) 130.